Spring 5-2-2011

Effects of Particle Properties on Cluster Characteristics in a 2-D CFB Riser

Jesse Zhu
Particle Technology Research Centre The University of Western Ontario, zhu@uwo.ca

Jing Xu
Particle Technology Research Centre The University of Western

EFFECTS OF PARTICLE PROPERTIES ON CLUSTER CHARACTERISTICS IN A 2-D CFB RISER

Jing Xu and Jesse Zhu*

Particle Technology Research Centre, Department of Chemical & Biochemical Engineering, The University of Western Ontario, London, Ontario, Canada N6A 5B9

*Corresponding author. Tel.: +1 519 661 3807; fax: +1 519 850 2441; email address: jzhu@uwo.ca (J. Zhu)

ABSTRACT

The characteristic of particle clusters was studied in a 2-D circulating fluidized bed riser by using a digital image system and optical fiber probes. A new parameter, cluster number fraction, was proposed to characterize the clusters. The results indicated the smaller and lighter particles have higher potential to aggregate, while the effects of particle sphericity were less significant than those of particle density and size.

INTRODUCTION

The analysis of the micro structure of the gas-solid two phases is considered complex and remains unclear. The micro flow structure is usually identified as the behavior of clusters, which are defined as dense clouds of particles having significantly more particles per unit volume than the surrounding dilute regions (1). Since the particles in CFB tend to aggregate and form clusters, which flow quite differently from a single particle, the gas-solid flow in CFBs is often characterized by the existence of particle aggregates or clusters (1, 2).

Most of the researchers (1-5) used the visualization technique and intrusive probe to obtain the micro flow behaviors. However, the visualization technique they used was restricted to dilute flow. In addition, almost all of the former studies appear to conduct the investigation within one type of particles, and very few references can be found clarifying the effects of particle properties on the cluster characteristics. Since previous studies (6, 7) have revealed that a strong dependence of the particle properties on the solids concentration and particle velocity, the particle properties, including particle density, size and sphericity may play an non-negligible role in affecting the cluster properties. In this study, various types of particles with typical different density, size or sphericity were taken into consideration. Moreover, very few studies have been carried out to investigate the cluster properties by combining the visualization with intrusive probes. In this study, we applied high-speed video camera and optic fiber probes in a 2-D circulating fluidized bed, to connect the two different measurements and make both function better. This study also realized the visualization technique to be effectively used under high solids concentration (G_s is up to 200 kg/m^{2}s).

EXPERIMENTAL APPARATUS

All experiments were carried out in a rectangular circulating fluidized bed which is illustrated schematically in Figure 1. The riser is a rectangular column with 7.6 m height and 19 mm × 114 mm (0.75 in × 4.5 in) cross-section.

The visualization system was self-designed and set up. To eliminate the entrance and exit effects, the system was mounted focusing on the upper fully developed region, where Z = 5m. The system consists of a light source, a high-speed video camera and programs for digital image analysis (Figure 2). The speed of the high-speed video camera is up to 16,000 fps. A MATLAB program was used to allow the images to be analyzed frame by frame. The probe chosen to measure the local solids concentration in this study was optical fiber probe, which is capable of measuring the solids concentration with a reliable pre-calibration (1, 8, 9). The solids concentrations were measured at 9 lateral positions and 6 axial levels along the entire riser. The instantaneous solids concentration was analyzed by a self-developed FORTRAN program which introduces sensitivity analysis to identify the clusters from solid concentration signals.

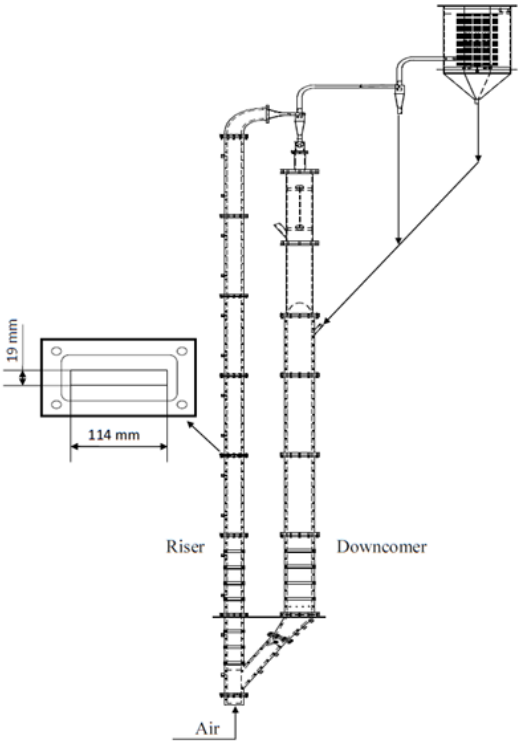

Figure 1 Circulating fluidized bed unit and schematic of riser cross section

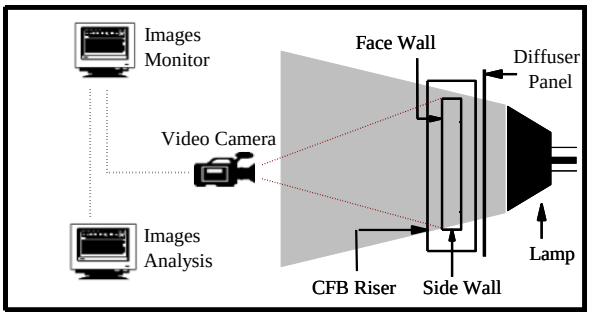

Figure 2 Sketch of Visualization system

The properties of the particles used in this study are listed in Table 1. The materials were selected in order to investigate the effects of particle size, density and sphericity, respectively. In this study, the solids concentration measurement was conducted under the operating conditions of U_g = 3 ~ 8 m/s, and G_s = 50 ~ 200 kg/m^2·s. The high-speed videos were recorded simultaneously under the corresponding operating conditions at 2000 fps.

Table 1 Properties of particles used

Particles	FCC	Glassbeads #1	Glassbeads #2	Glassbeads #3	Sand
Particle Sauter mean diameter, μm	67	76	134	288	138
Particle density, kg/m^3	1877	2453	2403	2498	2467
Bulk density, kg/m^3	1125	1434	1421	1475	1453
Sphericity, -	0.95	~1	~1	~1	0.65~0.75
Particle terminal velocity, m/s	0.26	0.42	1.19	3.73	N/A

RESULTS AND DISCUSSION

Observation and Description of Clusters

Generally, the solids flowing in the riser were observed to distribute dense in wall regions and dilute in the center. The particles were moving faster in the column center and slower towards the wall. Nearly no appearance of solids buildup or falling-down was observed on either of the face walls.

Cluster Forms

Figure 3 shows an image sequence with a solid cluster moving upwards in the center region of the riser. The frames (window size of 46.6 mm × 13.5 mm) were taken at a recording rate of 2000 fps and an exposure time of 500 μs. The movement and development of the cluster can be recognized as the darker structure which is visualized directly within the observed area. The sequence of images clearly show that a U-shape cluster is formed with a round nose facing downward and a core on the “nose tip”, where it is much darker than the peripheral area. Initially, the cluster is moving as a longish core with blurred boundary. Continuously, the core is stretched to be longer and crotched. Since the cluster is moving slower, the dispersed particles passing by are blocked and adhere to the cluster. Therefore, the U-shape outline is clearer and the core is darker and bigger with the aggregating of particles. In this study, the U-shape cluster is the most common form of clusters observed in the riser center.

As observed, the clusters exist as U-shape, longish strand and other cluster structures. The pictures of the clusters shown in Figure 4 are for different particles under several typical operating conditions. As mentioned above, the U-shape is the most common structure viewed in the riser center. Some of them have a core with particular high solids concentration at the nose tip, while the others don’t. The opening of the U-shape cluster faces upward or downward with a size range from 5 cm to 30 cm, most are smaller than 20 cm. The longish strand cluster is the cluster form also often observed in the core region of the riser. The size of the strand cluster is approximately 10 mm in width and 10 cm to 50 cm in length. The motion of this form of cluster is slower than other particles in the vicinity. Occasionally, some clusters in small size (1-2 cm), and in shapes of circle, short stripe (as shown in Figure 4(c)) or crescent are observed. They are always seen to flow as fast as the adjacent non-aggregative region. In addition, the shape of these types of clusters is nearly constant during the motion in the observation window. Besides the forms of individual clusters aforementioned, clusters in different structures may adhere

together to form floc-like clusters. The most common combination seen is between the U-shape and the strand clusters, typically shown in Figure 4(d), (e) and (f).

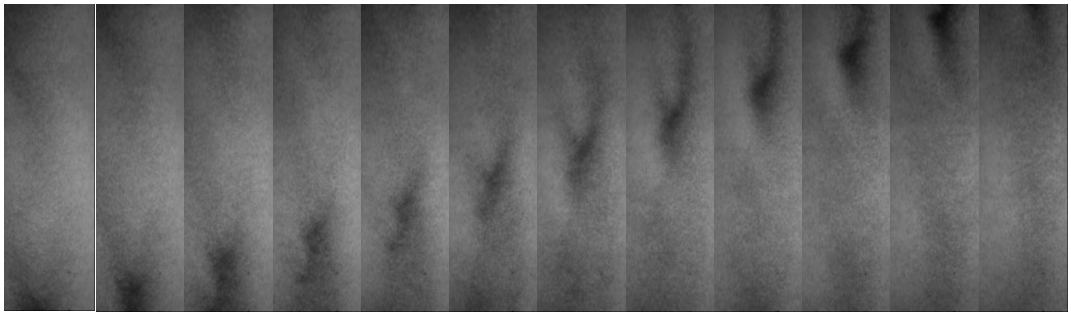

Figure 3 Sequence of 12 images taken in the core region with a U-shape cluster

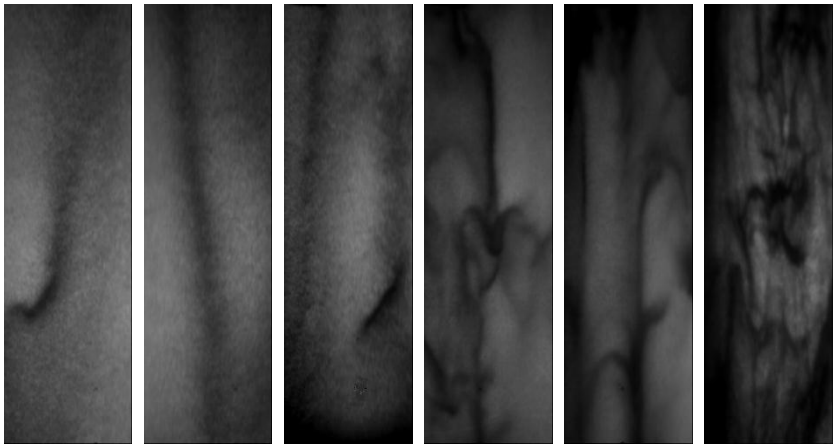

(a) (b) (c) (d) (e) (f)

Figure 4 Cluster structures observed in the riser center under different operating conditions: (a) Glassbead #3, G_s = 100 kg/m^2·s, U_g = 5 m/s; (b) Glassbead #3, G_s = 100 kg/m^2·s, U_g = 8 m/s; (c) Sand, G_s = 100 kg/m^2·s, U_g = 5 m/s; (d) Glassbead #1, G_s = 100 kg/m^2·s, U_g = 5 m/s; (e) Glassbead #1, G_s = 150 kg/m^2·s, U_g = 5 m/s; (f) FCC, G_s = 100 kg/m^2·s, U_g = 5 m/s

Effects of Particle Properties on Cluster Forms

Five different types of particles were employed in this study. The effects of particle density, size and sphericity on the clusters behaviors were compared. All the images in Figure 4 are in the size of 256 pixel ×880 pixel with a scale of 1.99×10^{-4} m/pixel. In Figure 4(a) and (b), Glassbead #3 with a mean size of 288 μm is seen to form clusters typically in U or strand shape and with a large cluster size. The Sand particles having particle diameter 134 μm and approximate 0.7 sphericity are observed to have the flow structure indistinguishable from the Glassbead #3, while small size clusters can be found occasionally. With further decreasing of particle size to 76 μm for Glassbead #1, the form of clusters turns to be more complicated and interconnective. It is seen that the clusters are smaller in size than that of the larger particles, and tend to connect together with each other. Therefore, the individual cluster is difficult to be identified in small size particle flow. Compared with the flow of Glassbead #1 (2453 kg/m^3), the structure of clusters is more intricate and irregular when lighter FCC particles (1877 kg/m^3) were used, as shown in Figure 4(f). The

area with darker color, which is occupied by the clusters, is obviously larger than the area in lighter color. In other words, - a great amount of particles are seen moving in aggregating form and few particles are left to move individually. The size and form of individual cluster is unlikely to be identified since the interconnection among the highly populated clusters is very intense. The observation indicates that the smaller and the lighter particles have higher potential to aggregate than the larger and heavier particles, whereas, the effect of particle sphericity cannot be distinguished here.

Characterizing Clusters with Optical Fiber Probe

To identify clusters with reflective probes applied, a set of criterion must be satisfied. Based on the previous studies, it is suggested that (3, 10): (1) the solids concentration inside the cluster must be *n*-times the standard deviation of the sampled signal over the local time-mean solids concentration; (2) the number of consecutive samples above the critical solids concentration, N_s, must be set to determine the minimum time interval for the perturbation caused by a cluster; (3) the sampling volume must be greater than one to two orders of particle diameter. Furthermore, it is found in this study that the sampling frequency of solids concentration signal is another sensitive criterion to establish the cluster properties. The sampling frequency in this study is placed very high, at 100 kHz, which allowed high sensitivity to the solids concentration.

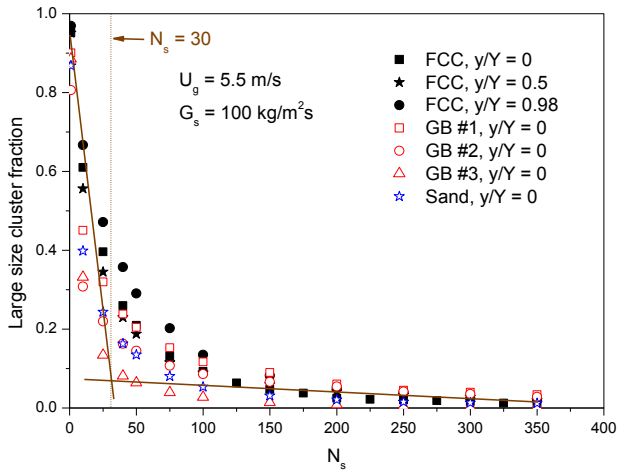

Figure 5 Cluster number fraction vs. N_s

Subjecting to the difference of sampling frequency among various studies, the optimal values for both *n* and N_s are required to be determined individually. The sensitivity analysis, firstly introduced by Manyele *et al.* (3), is adopted in this study to optimize the value for *n*. Consequently, *n*=2 is finalized as optimal critical solids concentration. Then, such method is further improved to identify N_s. A new parameter, cluster number fraction, F_{lc}, is proposed for the first time to characterize clusters. F_{lc} is defined as $F_{lc} = N_{lc}/N_c$, where N_c is the total number of perturbations with the solids concentration higher than the critical value over the time series studied; while N_{lc} is the number of perturbations with N_s consecutive samples above the critical solids concentration. Considering the cluster number fraction as a sample parameter for the sensitivity analysis, an increase/decrease of N_s would lower/raise the fraction of clusters with existence time longer than N_s sampling time interval.

Some of the perturbations of solids concentration are very small and with short time intervals, therefore, they are classified as part of the dispersed particulate phase. Since such small perturbations are numerous, there tends to be a decrease of F_{lc} with the increase of N_s. As shown in Figure 5, there is a sharp change at N_s = 30, which is the critical value that demarcates the particulate phase and the clusters. In addition, single critical N_s is also applicable to different types of particles and multiple lateral positions under specific operating condition.

Cluster Number Fraction (F_{lc})

It is found that F_{lc} can not only be used to determine the optimal value for N_s, but also characterizes the effects of particle properties on the aggregates. Since N_s is the number of consecutive samples, with a sampling frequency, it can be easily transfromed to the minimum time interval, T_c, set for the perturbation caused by a cluster.

Since the clusters are irregular in shape and vary both laterally and axially within a riser, the accurate definition of the cluster size is impossible. Therefore, the vertical length is usually used to identify the size of clusters. Since the time interval of the solids concentration perturbation measured by the optical fiber probe represents the traveling time of a cluster passing through a probe tip, it is feasible to calculate the cluster vertical length with $d_{vl} = V_c \times T_c$, where V_c is the vertical velocity of cluster (11). With the evaluation of the cluster velocity, it is possible to obtain the size of clusters in the riser. To some extent, the cluster number fraction reflects the distribution of cluster size.

Figure 6 plots F_{lc} against minimum time interval to elucidate the cluster characteristics of different particles. Figure 6(a) interprets the fractions of cluster number at different lateral positions. The F_{lc} at the riser center region (y/Y = 0), middle region (y/Y = 0.5) and wall region (y/Y =0.98) are seen decrease with the increase of minimum time interval. In other words, with increasing T_c set for a cluster, the number of clusters with the transit time longer than the criterion decreases. It can also be seen that the decreasing curves of y/Y =0 and y/Y = 0.5 are almost overlapping and cross approximately at $T_c = 1.1\times10^{-3}$ μs. Below this value, the cluster number fraction at y/Y =0 is larger than that at y/Y = 0.5, while smaller when beyond the point. The curve for the wall region with y/Y = 0.98 is obviously above the other two, meaning that the population of clusters in the wall region is larger than that in the center or middle region. Due to the wall friction, the particle velocity is low on the wall, which increases the tendency of forming clusters and the probability of existence for clusters.

Figure 6(b) compares F_{lc} of particles with different mean size. It is found that under identical T_c, the F_{lc} of smaller size particles is greater than that of larger particles. It shows that the finer particles are prone to aggregate and incline to form clusters. It is agreed well with the observations in the section 3.2. The finer particles (GB #1 or FCC particles) were seen to form numerous clusters interconnecting with each other, while only several huge size clusters were observed occasionally in the coarse particles (GB #3 or Sand).

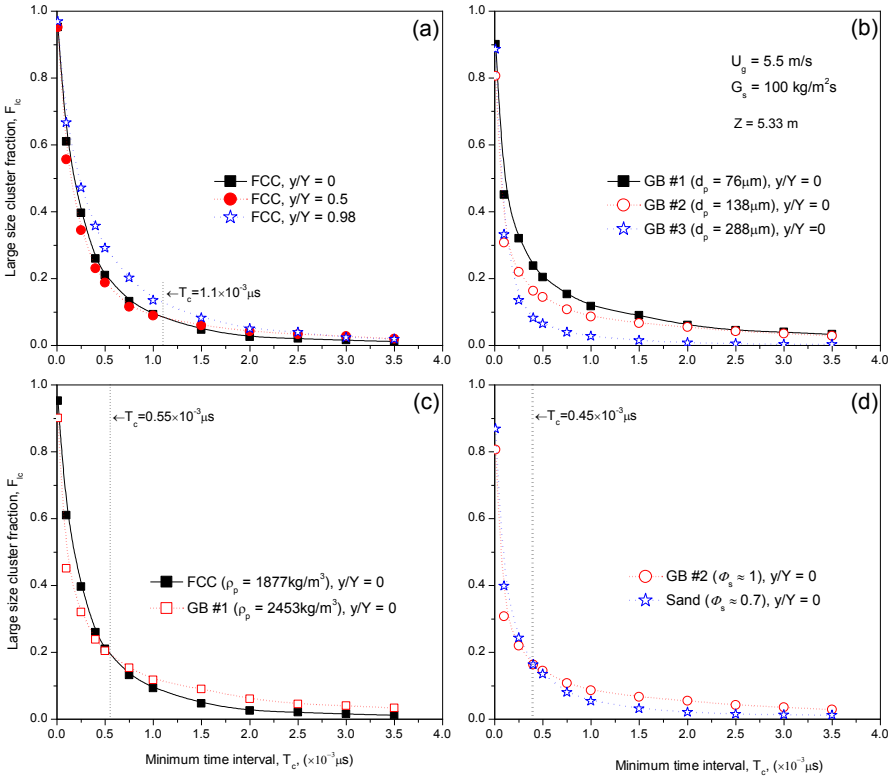

Figure 6 Cluster number fraction for different particles.

For the particles with different density, the curves of F_{lc} against T_c cross approximately at $T_c = 0.55\times10^{-3}$ μs, as the dotted line shown in Figure 6(c). Under the given small time criterion, the fraction of clusters number for FCC particles is larger than that of GB#1. With the increase of T_c, the clusters for heavier particles (GB #1) are greater in fraction than for lighter particles (FCC) when T_c passes over the marked dotted line. It indicates that the lighter particles tend to form smaller clusters than the heavier particles. It is matched with the observations by high-speed films in section 3.2.

The curves for particles with different sphericities are also observed in Figure 6(d) when $T_c = 0.45\times10^{-3}$ μs. Same interpretation can also be applied to the different sphericities particles: the more spherical particles incline to aggregate larger size clusters than the irregular particles when T_c is beyond the value of the intersection point. Below the marked line, the two curves are nearly overlapping, indicating that the clusters fraction in each cut for both types of particles are almost the same. In other words, the sphericity of particles has only minor effects on the small size clusters but more obvious effects on the larger size clusters.

CONCLUSION

The particle aggregation characteristics were studied in a narrow rectangular CFB riser with a 19 mm × 114 mm cross-section and a 7.6m length. The study was conducted by operating FCC, glassbeads and sand particles under various operating conditions. Forms of clusters were observed by employing a visualization system with a high-speed video camera. The lighter and smaller particles tended to

aggregate and form interconnected clusters, while the effects of particle sphericity on the form of clusters are less evident. The aggregation characteristics were also studied with the optical fiber probe. A new parameter, the cluster number fraction, was originally defined. The results obtained by analyzing the instantaneous solids concentration agreed well with the observations and also indicate that the low particle density and small particle size contribute to form clusters. It shows that the particle sphericity plays a limited role in affecting the particle aggregation.

NOTATION

d_p Sauter mean diameter of particle, m
d_{vl} Cluster vertical length, m
F_{lc} Cluster number fraction
G_s Solids circulation rate, kg/m^2·s
T_c Minimum time interval for cluster, s
U_g Superficial gas velocity, m/s
V_c Cluster vertical velocity, m/s
Y Half of riser width, m
y Lateral coordinates
N_{lc} Number of clusters
N_c Number of perturbations higher than critical solids concentration
N_s Number of consecutive samples above critical solids concentration
Z Height from riser bottom, m
ρ_p Density of particle, kg/m^3
Φ_s Particle sphericity

REFERENCES

1. Bi, H.T., J.X. Zhu, Y. Jin, and Z.Q. Yu. Forms of particle aggregations in CFBs. in Proceedings of the Sixth Chinese Conference on Fluidization. 1993. Wuhan, China.
2. Soong, C.H., K. Tuzla, and J.C. Chen. Experimental determination of cluster size and velocity in circulating fluidized bed. in Fluidization VIII. 1995. New York: Engineering Foundation.
3. Manyele, S.V., J.H. Pärssinen, and J.-X. Zhu, Characterizing particle aggregates in a high-density and high-flux CFB riser. Chemical Engineering Journal, 2002. 88: p. 151-161.
4. Li, H., Y. Xia, Y. Tung, and M. Kwauk, Micro-visualization fo clusters in a fast fluidized bed. Powder Technology, 1991. 66: p. 231-235.
5. Hatano, H. and N. Kido, Microscope visualization of solid particles in circulating fluidized beds. Powder Technology, 1994. 78: p. 115-119.
6. Mastellone, M.L., U. Arena, The effect of particle size and density on solids distribution along the riser of a circulating fluidized bed. Chemical Engineering Science, 1999. 54: p. 5383-5391.
7. Xu, J. and J. Zhu, Effects of particle properties on flow structure in a rectangular circulating fluidized bed: solids concentration distribution and flow development. Submitted to Chemical Engineering Science, 2011.
8. Zhang, H., P.M. Johnston, J.-X. Zhu, H.I. de Lasa, and M.A. Bergougnou, A novel calibration procedure for a fiber optic solids concentration probe. Powder Technology, 1998. 100: p. 260-272.
9. Liu, J., J.R. Grace, and X. Bi, Novel multifunctional optical-fiber probe I: Development and validation. AIChE Journal, 2003. 49: p. 1405-1420.
10. Soong, C.H., K. Tuzla, and J.C. Chen. Identification of particle clusters in circulating fluidized bed. in Circulating Fluidized Bed Technology IV. 1994. New York: AIChE.
11. Li, H., Q. Zhu, H. Liu, and Y. Zhou, The cluster size distribution and motion behavior in a fast fluidized bed. Powder Technology, 1995. 84: p. 241-246.